# Lead-207 NMR: A Novel Probe for the Study of Calcium-Binding Proteins

**Article** *in* JBIC Journal of Biological Inorganic Chemistry · February 1996

DOI: 10.1007/s007750050021

CITATIONS
28

READS
112

**6 authors**, including:

James M Aramini
City University of New York - Advanced Science Research Center
**105** PUBLICATIONS **3,601** CITATIONS
SEE PROFILE

Tianbao Yuan
University of Toronto
**19** PUBLICATIONS **1,424** CITATIONS
SEE PROFILE

Hans J Vogel
The University of Calgary
**531** PUBLICATIONS **20,284** CITATIONS
SEE PROFILE

JBIC (1996) 1:39–48 

ORIGINAL ARTICLE

**James M. Aramini · Toshifumi Hiraoki
Michio Yazawa · Tao Yuan · Mingjie Zhang
Hans J. Vogel**

# Lead-207 NMR: a novel probe for the study of calcium-binding proteins

**Abstract** The high-affinity $Ca^{2+}$–binding sites of carp (pI 4.25) and pike (pI 5.0) parvalbumins, as well as those of mammalian calmodulin (CaM) and its C-terminal tryptic half-molecule ($TR_2C$), were analyzed by $^{207}Pb$ NMR spectroscopy. For the parvalbumins, two $^{207}Pb$ signals were observed ranging in chemical shift from $\approx$750 to $\approx$1260 ppm downfield of aqueous $Pb(NO_3)_2$, corresponding to $^{207}Pb^{2+}$ bound to the two high-affinity helix-loop-helix $Ca^{2+}$–binding sites in each of these proteins. Four $^{207}Pb$ signals, which fall in the same chemical shift window, could be discerned for CaM. Experiments on $TR_2C$ permitted the assignment of each signal as due to $^{207}Pb^{2+}$ occupying a helix-loop-helix site in either the N- or the C-lobe of the intact protein. $^{207}Pb$ and $^{1}H$ NMR titration studies on CaM provided evidence that $Pb^{2+}$ binding to all four sites occurs simultaneously, in contrast to the behavior of this protein in the presence of $Ca^{2+}$. Titrations of the $^{207}Pb^{2+}$–forms of CaM and $TR_2C$ with the antipsychotic drug trifluoperazine demonstrated that drug binding to the exposed hydrophobic surfaces in CaM causes substantial conformational changes and proceeds in a sequential manner – first the C-lobe and subsequently the N-lobe. Finally, the field dependence of CaM-bound $^{207}Pb$ signals was examined. The $^{207}Pb$ signal linewidths exhibited a sharp dependence on the square of the external magnetic field, a trend characteristic of relaxation via chemical shift anisotropy. Relaxation studies on $TR_2C$ demonstrated that chemical exchange also contributes to the observed linewidths. The large chemical shift dispersion observed for the $^{207}Pb$ signals of the three proteins studied here illustrates the remarkable sensitivity of this parameter to subtle differences in the chemical environment of the protein-bound $^{207}Pb$ nucleus. To our knowledge, the data presented in this article comprise the first ever published example of the application of $^{207}Pb$ NMR spectroscopy to metalloproteins.

**Key words** $^{207}Pb$ NMR · Calmodulin · Parvalbumin · Helix-loop-helix

Presented in part at the Eighth International Symposium on Calcium-Binding Proteins and Calcium Function in Health and Disease, 23–27 August 1992, Davos, Switzerland

J.M. Aramini · T. Yuan · M. Zhang[1] · H.J. Vogel (✉)
Department of Biological Sciences, University of Calgary, Calgary, Alberta, Canada T2N 1N4
Tel. +1-403-220 6006; Fax +1-403-289 9311;
e-mail vogel@acs:ucalgary.ca

T. Hiraoki
Department of Applied Physics, Hokkaido University, Sapporo 060, Japan

M. Yazawa
Department of Chemistry, Hokkaido University, Sapporo 060, Japan

[1]*Present address*: Department of Biochemistry, Hong Kong University of Science and Technology, Clear Water Bay, Kowloon, Hong Kong

## Introduction

Because few metals rival calcium in terms of the wide variety of physiological processes on which it exerts some influence, considerable attention has been focused on elucidating the structures and functions of proteins which bind $Ca^{2+}$. This research constitutes a major tenet in the field of biological inorganic chemistry [1, 2]. $Ca^{2+}$–binding proteins can be categorized on the basis of their biological functions and the manner in which they sequester calcium ions [3, 4]. The best known are the intracellular helix-loop-helix $Ca^{2+}$–binding proteins, which include calmodulin (CaM), parvalbumin (Pa), troponin C, and calbindin $D_{9K}$. These proteins share a common $Ca^{2+}$–binding motif – termed "helix-loop-helix" or "EF-hand" – characterized by two $\alpha$-helices flanking a loop of 12 residues; such sites almost invariably occur in tandem, with

**Table 1** Partial amino acid sequences for the $Ca^{2+}$-binding loops in carp (pI 4.25) Pa, pike (pI 5.0) Pa, and mammalian CaM. Source of sequences: carp (pI 4.25) Pa [7, 8]; pike (pI 5.0) Pa [9]; CaM [13, 14]

| Protein | Site | Position in loop[a] | | | | | |
|---|---|---|---|---|---|---|---|
| | | X | Y | Z | −Y | −X | −Z |
| Carp (pI 4.25) Pa | CD | $D^{51}$ | D | S | *F* | E | **E** |
| | EF | $D^{90}$ | D | D | *K* | $H_2O$ | **E** |
| Pike (pI 5.0) Pa | CD | $D^{51}$ | D | S | *F* | E | **E** |
| | EF | $D^{90}$ | D | D | *K* | $H_2O$ | **E** |
| Mammalian CaM | I | $D^{20}$ | D | D | *T* | $H_2O$ | **E** |
| | II | $D^{56}$ | D | N | *T* | $H_2O$ | **E** |
| | III | $D^{93}$ | D | N | *Y* | $H_2O$ | **E** |
| | IV | $D^{129}$ | D | D | *Q* | $H_2O$ | **E** |

[a] Modes of ligand binding to the metal ion: *normal letters* monodentate binding via side-chain carboxylate, carbonyl, or hydroxyl moieties, *italic letters* binding via main-chain carbonyl, *bold letters* bidentate binding via side-chain carboxylate. The *superscripts* denote the sequence positions of the first residue in each of the sites

the metal ions separated by a short anti-parallel $\beta$-sheet [5, 6]. The residues that participate in coordinating the calcium ion originate from highly conserved positions in the $Ca^{2+}$–binding loop: residues 1, 3, 5, 7, 9, and 12 (denoted as coordination positions X, Y, Z, -Y, -X, and -Z). The primary sequences for the loops in the proteins relevant to this study, carp (pI 4.25) and pike (pI 5.0) Pa and mammalian CaM, are given in Table 1.

The parvalbumins are small (MW $\approx$11.5 kDa) acidic proteins found in vertebrate muscle tissues. Although their function remains somewhat obscure [3], they possess two high-affinity ($K_D \approx 10^{-9}$ M) EF-hand $Ca^{2+}$–binding sites. Recently refined X-ray crystal structures of carp (pI 4.25) Pa revealed that the $Ca^{2+}$ ions in both the CD and EF sites of the protein are chelated by seven oxygen atoms, although the sites are geometrically distinct (pentagonal bipyramid vs monocapped trigonal prism) [7, 8]. In addition, all seven $Ca^{2+}$ ligands in the CD site are furnished by the protein, whereas the -X position in the other site is occupied by a water molecule (a common occurrence in other helix-loop-helix sites [6]). The primary structures of the $Ca^{2+}$–loops in carp (pI 4.25) and pike (pI 5.0) Pa are highly conserved; hence, in the absence of a highly refined three-dimensional structure for this protein [9], we assume that the CD and EF sites in the two parvalbumins are homologous.[1]

[1] An unpublished 1.65-Å resolution X-ray crystal structure of the $Ca^{2+}$ form of pike (pI 5.0) Pa by J.P. DeClercq, B. Tinant, F. Roquet, J. Rambauld, and J. Parello has recently appeared in the Protein Data Bank (Brookhaven National Laboratories, Upton, N.Y.). There appears to be a high degree of homology between the helix-loop-helix $Ca^{2+}$–binding sites in this protein and carp (pI 4.25) Pa.

Calmodulin is a small (MW $\approx$ 16.8 kDa) ubiquitous eukaryotic protein which, in response to minute changes in $Ca^{2+}$ levels within the cell, can bind to a variety of intracellular target proteins and enzymes, thereby mediating a multitude of biological events [10, 11]. X-ray structures of CaM have demonstrated that the protein is bilobal, with each lobe containing a juxtaposed pair of high-affinity ($K_D \approx 10^{-5}$–$10^{-6}$ M) $Ca^{2+}$–binding sites. The two lobes are separated by a short $\alpha$-helical linker [12–14].The four EF-hand sites in the protein are each comprised of four side-chain carboxylates (X, Y, Z, -Z), one of which binds in a bidentate fashion (-Z), a main-chain carbonyl (-Y), and a water molecule (-X). The seven oxygen ligands in each site are arranged in a distorted pentagonal bipyramidal geometry around the metal ion.

Along with X-ray crystallographic studies, nuclear magnetic resonance (NMR) spectroscopy has proven to a be powerful tool for gaining insight into the structures and dynamics of helix-loop-helix $Ca^{2+}$–binding proteins. Both $^{43}Ca$ [15, 16] and $^{113}Cd$ [16–18] have been successfully employed as high-affinity probes for the helix-loop-helix sites in this class of proteins. In this paper, we introduce the study of another surrogate metal ion, $Pb^{2+}$, in place of $Ca^{2+}$, and examine its binding to parvalbumins and calmodulin by $^{207}Pb$ NMR spectroscopy, an approach that has never been applied to metalloproteins. Although the ionic radius of $Pb^{2+}$ is somewhat larger than those of $Ca^{2+}$ and $Cd^{2+}$, which are quite similar in size [19], $^{207}Pb$ exhibits several appealing traits, including a moderate resonance frequency, a vast chemical shift range and potentially large spin-spin couplings to neighboring nuclei, in comparison to the traditional probes (Table 2) [20, 21]. The toxicological properties of lead have spurred a number of investigations into the interactions of this metal ion with various proteins (for a recent review, see [22]). For example, it has been demonstrated that $Pb^{2+}$ can bind very tightly to, and even displace $Ca^{2+}$ from, CaM, calbindin, and troponin C [23]. Moreover, $Pb^{2+}$ can substitute for $Ca^{2+}$ in the activation of several enzymes, including protein kinase C [24], phosphodiesterase [25], and myosin light chain kinase [26], the latter two in a calmodulin-dependent manner. These traits of lead make the biological application of $^{207}Pb$ NMR all the more relevant.

**Table 2** Relevant NMR parameters of $^{43}Ca$, $^{113}Cd$, and $^{207}Pb$. NMR parameters obtained from [15, 17, 20, 21]. *I* Nuclear spin, $\nu_0$ nuclear resonance frequency, *R(/$^{13}$C)* receptivity with respect to $^{13}C$, $\delta$ chemical shift

| Nucleus | $r$(Å)[b] $M^{2+}$ | I | Natural abundance | $\nu_0$(11.7 T) (MHz) | $R$(/$^{13}$C) | $\delta$ range (ppm) |
|---|---|---|---|---|---|---|
| $^{43}Ca$ | 1.00 | 7/2 | 0.145 | 33.6 | 0.053 | ≈60 |
| $^{113}Cd$ | 0.95 | ½ | 12.3 | 110.9 | 7.6 | ≈900 |
| $^{207}Pb$ | 1.19 | ½ | 22.6 | 104.4 | 11.7 | ≈16000 |

[a] Six-coordinate ionic radii ($r$) obtained from [19]

## Materials and methods

### Materials

Carp (pI 4.25) and pike (pI 5.0) parvalbumins were purified from their respective sources according to published methods with a minor modification [27, 28]. These proteins were decalcified by precipitation with trichloroacetic acid, followed by dialysis in the presence of $\beta$-mercaptoethanol ($\approx$1 mM), and ultimately lyophilization [28, 29]. CaM was isolated from bovine testis (Pel-Freez Biologicals) and an *Escherichia coli* expression system following standard literature procedures [30]. The proteins from these sources are identical in every respect except that bacterial CaM lacks N-acetylation and a trimethyllysine at position 115. The C-terminal half-molecule of CaM ($TR_2C$; 78–148) was obtained by mild digestion with l-1-tosylamido-2-phenylethyl chloromethyl ketone (TPCK)-treated pancreatic trypsin (Sigma) and purified as previously described [31, 32]. The apo-forms of CaM and $TR_2C$ were generated by passing the proteins down a small Chelex-100 column, equilibrated in 50 mM $NH_4HCO_3$ pH 8.5, followed by lyophilization. For each apoprotein, the amount of residual $Ca^{2+}$ present was less than 0.05 mol equiv, as judged by $^1$H NMR. All proteins were stored in a lyophilized form at –20 °C prior to use.

Potassium chloride was obtained from Aldrich, piperazine-*N–N′-bis*[ethanesulfonic acid] (PIPES) and trifluoperazine from Sigma. Isotopically enriched $^{207}Pb(NO_3)_2$ (91.6%) and $^{113}CdO$ (94.8%) were purchased from Oak Ridge National Laboratories and MSD Isotopes, respectively. Stock solutions of $^{207}Pb(NO_3)_2$ and $^{113}Cd(ClO_4)_2$ [33], each 0.1 M in $D_2O$ (Cambridge Isotope Laboratories), were used as titrants as well as chemical shift references in $^{207}$Pb and $^{113}$Cd NMR experiments.

### Sample preparation

Samples for NMR analysis were prepared by dissolving each protein in $\approx$2.0 ml of 25% v/v $D_2O$ containing 0.1 M KCl (unless otherwise specified). For the Pa work, the solutions were also buffered (20 mM PIPES). All sample manipulations were performed using acid-washed glassware and plasticware to minimize recalcification. The concentrations of all protein solutions were determined spectrophotometrically using the following extinction coefficients: carp Pa (pI 4.25), $_{259}$ = 2020 $M^{-1}cm^{-1}$ [34]; pike Pa (pI 5.0), $_{258}$–$e_{268}$ = 918 $M^{-1}cm^{-1}$ [35]; CaM, $_{276}$(1%) = 1.8 $cm^{-1}$ [36]; $TR_2C$, $_{276}$ = 3006 $M^{-1}cm^{-1}$ [37]. The pH of each sample was adjusted to the desired value as detailed in our earlier studies [38].

### NMR spectroscopy

All NMR data presented in this paper were recorded locked and at 25 °C.

$^{207}$Pb NMR spectra were acquired at a resonance frequency of 104.435 MHz on a Bruker AMX 500 instrument equipped with a 10-mm broadband probe. The following acquisition parameters were employed: 60–80° pulses, a sweep width of 100 kHz, 0.40–0.55 s between pulses, and 16 K data points. Data were left shifted to give an effective dead time of 50–70 μs, zero-filled once, and processed with an exponential line broadening of 150–250 Hz. For the field-dependent studies, $^{207}$Pb NMR spectra were also obtained on Bruker AM 400, AC 300 (Bruker Canada, Milton, Ont.), and WP 100 (Simon Fraser University, Burnaby, B.C.) instruments at resonance frequencies of 83.55, 62.66, and 20.89 MHz, respectively, using conditions similar to those outlined above. Protein-bound $T_1$ measurements were performed on the AM 400 spectrometer, using the progressive saturation approach [21], and analyzed with standard Bruker software. All $^{207}$Pb NMR spectra are referenced to external 0.10 M $^{207}Pb(NO_3)_2$ in $D_2O$.[2]

$^1$H NMR spectra were obtained at a resonance frequency of 500.139 MHz on a Bruker AMX 500 instrument equipped with a 5-mm $^1$H probe, using 90° pulses, a 6000-Hz sweep width, a 2.7-s repetition time, 8 K data points, and presaturation of the residual HDO signal. The data were zero-filled once and processed with a 2-Hz line broadening. $^1$H NMR spectra are referenced to internal sodium 2,2-dimethyl-2-silapentane-5-sulfonate (DSS; MSD Isotopes).

$^{113}$Cd NMR measurements were conducted on Bruker AMX 500 and AM 400 NMR instruments (using 10-mm broadband probes) at resonance frequencies of 110.92 and 88.75 MHz, respectively. Typical acquisition parameters were as follows: 50–70° pulses, a 30-kHz sweep width, 0.5–0.6 s between pulses, and 4–8 K data points. Data were zero-filled to 16 K prior to Fourier transformation with an exponential line broadening of 30–40 Hz. All $^{113}$Cd spectra are referenced to external 0.10 M $^{113}Cd(ClO_4)_2$ in $D_2O$.

Linewidths of protein-bound $^{207}$Pb and $^{113}$Cd NMR signals were calculated by the "ldcon" routine (UXNMR); for overlapping resonances, the LINESIM program (DISNMR; P. Barron, Bruker, Australia) was used.

## Results and discussion

### $^{207}$Pb NMR studies of parvalbumins

$^{207}$Pb NMR spectra of $^{207}Pb^{2+}$ saturated pike (pI 5.0) and carp (pI 4.25) parvalbumins are shown in Fig. 1. For both proteins, one observes two $^{207}$Pb signals which correspond to the metal ion bound to the two high-affinity EF-hand $Ca^{2+}$–binding sites (CD and EF) of these molecules. Note that in both cases the protein-bound $^{207}$Pb signals for the highly homologous sites are very well separated (i.e., by $\approx$350–450 ppm) (Table 3). This observation illustrates the extremely high sensitivity of the $^{207}$Pb chemical shift to subtle differences in the chemical environment of the nucleus, in stark contrast to the $^{113}$Cd NMR data for these proteins, where the protein-bound $^{113}$Cd peaks are separated by merely a few ppm (carp Pa: CD $\delta$ = –93.8 ppm, EF $\delta$ = –97.5 ppm; pike Pa: CD $\delta$ = –87.5 ppm, EF $\delta$ = –90.2 ppm) [35, 39].

To confirm that the signals observed above for the two parvalbumins are indeed due to $^{207}Pb^{2+}$ occupying the CD and EF sites of these proteins, we performed a $Ca^{2+}$ back titration of pike Pa (Fig. 2). Addition of $Ca^{2+}$ results in the attenuation and eventual disappearance of the $^{207}$Pb signals, although the latter can only be accomplished with a significant excess of $Ca^{2+}$. This suggests that the relative affinities of these metal ions for pike Pa are quite comparable. Furthermore, over the course of the titration, the protein-bound $^{207}$Pb re-

[2] The $^{207}$Pb chemical shift reference used in this work resonates 19.8 ppm downfield from the secondary reference 1.0 M $Pb(NO_3)_2$ in $H_2O$ whose chemical shift is –2961.2 ppm with respect to the accepted reference for this nucleus, 80% $Pb(CH_3)_4$ in toluene [see 20].

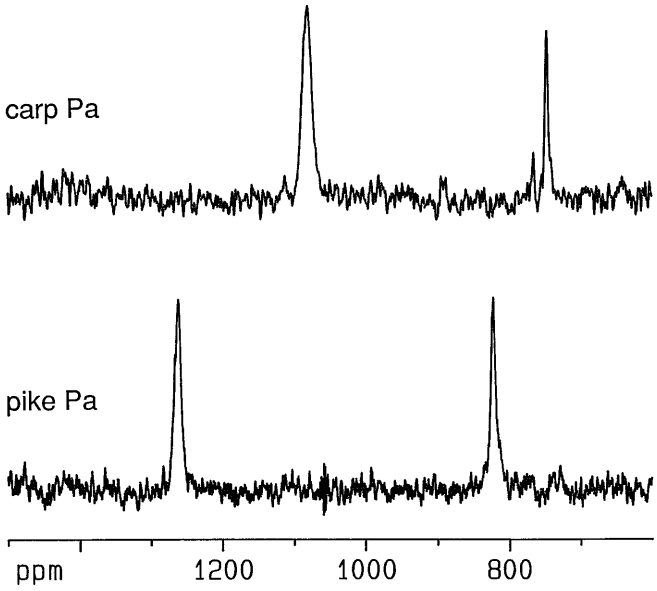


**Fig. 1** $^{207}Pb$ (104.435 MHz) NMR spectra of the $^{207}Pb^{2+}$ forms of pike (pI 5.0) and carp (pI 4.25) Pa (*pike Pa* 1.67 mM, 2.0 equiv $^{207}Pb^{2+}$, 20 mM PIPES, 100 mM KCl, pH 6.8, 39000 scans; *carp Pa* 1.96 mM Pa, 2.0 equiv $^{207}Pb^{2+}$, 20 mM PIPES, 100 mM KCl, pH 6.9, 100000 scans). Note that the incorrect relative areas obtained in the carp Pa spectrum are due to the spectrometer offset; the correct intensity ratios are found when the carrier is positioned between the resonances (data not shown)

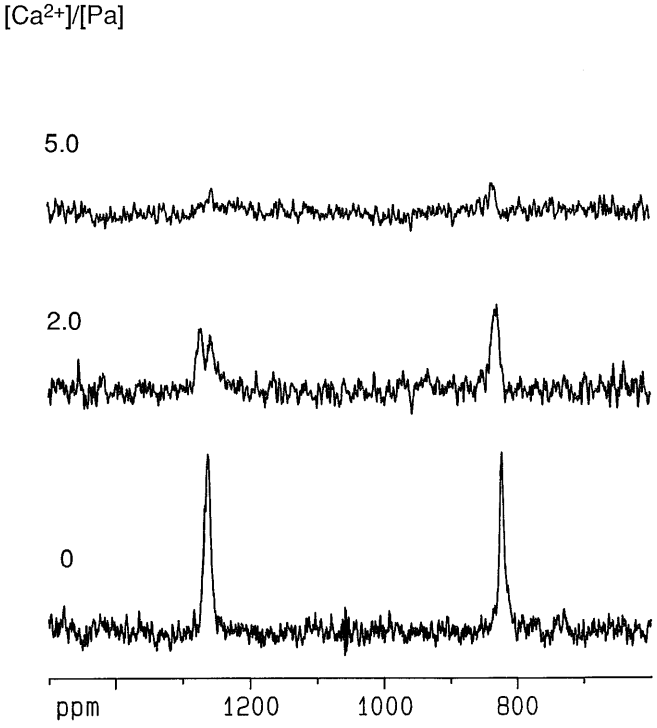


**Fig. 2** $^{207}Pb$ (104.435 MHz) NMR spectra of the back titration of 1.67 mM $(^{207}Pb)_{2.0}$ pike Pa with $Ca^{2+}$ (equiv $Ca^{2+}$: *0* pH 6.8, 39000 scans, *2.0* pH 7.1, 40000 scans, *5.0* pH 7.0, 20000 scans)

**Table 3** $^{207}Pb$ NMR data ($B_0 = 11.7$ T) for pike Pa (pI 4.25) and carp Pa (pI 5.0), mammalian CaM, and $TR_2C$

| Protein | δ (ppm) | $\Delta\nu_{1/2}$ (Hz) | Site |
|---|---|---|---|
| $(^{207}Pb^{2+})_{2.0}$Pa (pike) | 1262 | 870 | CD[a] |
| | 822 | 700 | EF[a] |
| $(^{207}Pb^{2+})_{2.0}$Pa (carp) | 1081 | 1200 | CD[a] |
| | 747 | 390 | EF[a] |
| $(^{207}Pb^{2+})_{4.0}$CaM | 1082 | 1150 | III/IV |
| | 1000 | 1550 | I/II |
| | 980 | 1050 | III/IV |
| | 899 | 2000 | I/II |
| $(^{207}Pb^{2+})_{2.0}TR_2C$ | 1084 | 1000 | III/IV |
| | 980 | 840 | III/IV |
| $(^{207}Pb^{2+})_{4.0}CaM(TFP)_{2.0}$ | 1174 | 2100 | III/IV |
| | 983 | 1200 | III/IV |
| | 965 | 820 | I/II |
| | 854 | 2100 | I/II |
| $(^{207}Pb^{2+})_{2.0}TR_2C(TFP)_{1.0}$ | 1187 | 970 | III/IV |
| | 981 | 720 | III/IV |

[a] Tentative assignments (see text)

sonances undergo appreciable shifts (upto 10 ppm) and a third resonance is discernable. This behavior is most likely due to the transient formation of hybrid species $[Pa(Ca)_{CD}(Pb)_{EF}$ and $Pa(Pb)_{CD}(Ca)_{EF}]$ and to the sensitivity of each site to the nature of the metal ion occupying the adjacent site, owing to their close proximity and the presence of a hydrogen-bonded antiparallel β-sheet between them. Analogous intersite interactions have been observed with $^{113}Cd$ NMR in lanthanide competition experiments on the $^{113}Cd$ forms of carp and pike Pa [34, 40], and in studies of other EF-hand $Ca^{2+}$–binding proteins (i.e., calbindin $D_{9K}$ [41]; CaM, see below). In order to assign the $^{207}Pb$ signals observed for both parvalbumins, one can exploit the differences in the relative affinities of the CD and EF sites in these proteins for various lanthanides and the numerous factors which perturb the CD sites due to the presence of a weak secondary metal ion binding site in its vicinity [34, 35, 40, 42]. For example, we found that back titration of $(^{207}Pb^{2+})_2$–pike Pa with $Lu^{3+}$, which is known to bind preferentially to the EF site of parvalbumins, displaced the high-field $^{207}Pb$ signal (data not shown). Thus, we assigned the low- and high-field $^{207}Pb$ signals for pike Pa, and, by inference, for carp Pa, to $^{207}Pb^{2+}$ bound to the CD and EF sites, respectively.

## $Pb^{2+}$ binding to bovine CaM and $TR_2C$

Figure 3 shows the titration of mammalian apo-CaM with $^{207}Pb$-enriched lead nitrate followed by $^{207}Pb$ NMR. Four signals are observed in the same spectral window as that employed for the studies of the parvalbumins. Moreover, these signals increase in intensity up to 4.0 equiv of metal ion, indicating that all four EF-

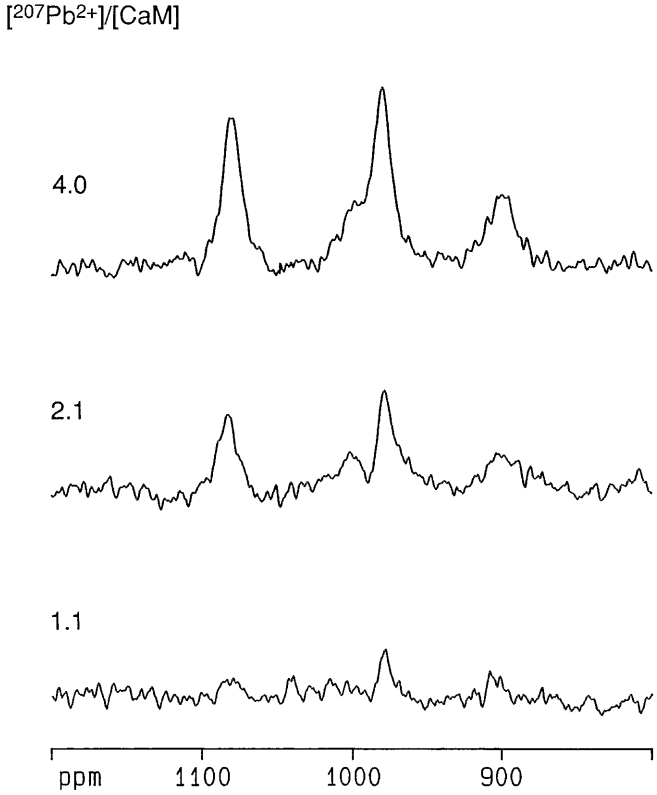


**Fig. 3** $^{207}Pb$ (104.435 MHz) NMR spectra of the titration of 1.47 mM bacterially expressed mammalian apo-CaM (100 mM KCl, pH 7.1) with $^{207}Pb^{2+}$; 85000 scans each. Note that the effective dead time used in data processing attenuates the broader resonances in the spectrum, altering the observed relative intensities

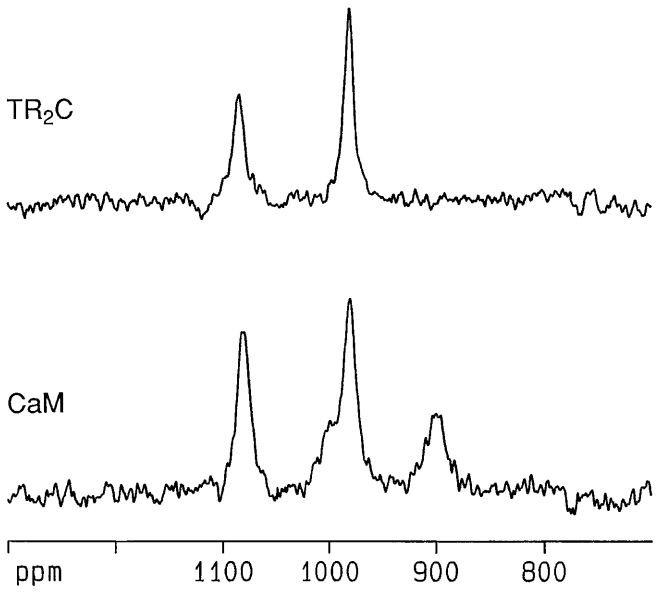


**Fig. 4** $^{207}Pb$ (104.435 MHz) NMR spectra of the $^{207}Pb^{2+}$ forms of bacterially expressed mammalian CaM (1.47 mM, 4.0 equiv $^{207}Pb^{2+}$, 100 mM KCl, pH 7.1, 85000 scans) and its C-terminal domain fragment, $TR_2C$ (1.11 mM, 2.0 equiv $^{207}Pb^{2+}$, 100 mM KCl, pH 7.0, 80000 scans)

hand binding sites of CaM are saturated in a concerted fashion by $^{207}Pb^{2+}$. The four signals can be assigned to the respective domains of the protein by analysis of proteolytic fragments of CaM, a strategy that has been routinely used in $^{1}H$ and $^{113}Cd$ NMR studies of this protein [31, 32, 43, 44]. Such investigations, as well as circular dichroism [45] and Fourier transform infrared studies [46], have shown the preservation of structure in the isolated N- and C-terminal tryptic fragments of CaM. As shown in Fig. 4, the $^{207}Pb$ signals at $\delta = 1082$ and 980 ppm in the intact protein line up almost perfectly with the two resonances observed for the $^{207}Pb^{2+}$ form of the C-terminal tryptic half-molecule of CaM ($TR_2C$; residues 78–148). Thus, by inference, the two broader signals in Fig. 3 ($\delta = 1000$ and 899 ppm) can be assigned to sites I and II in the protein. The $^{207}Pb$ NMR data for CaM and $TR_2C$ are given in Table 3.

The simultaneous binding of $Pb^{2+}$ to the four EF-hand $Ca^{2+}$–binding sites of bovine CaM can be confirmed by monitoring the conformational changes associated with metal ion binding to these sites by $^{1}H$ NMR. Figure 5 shows the aromatic region of the $^{1}H$ NMR spectrum of apo-CaM during a $Pb^{2+}$ up-titration. In general, the signals corresponding to residues in the C-terminal lobe undergo changes that are indicative of slow exchange binding to sites III and IV of the protein. For example, the and $\delta$ aromatic protons of Y138 ($\delta = 6.70$ and 6.66 ppm) in the apoprotein decrease in intensity over the course of the titration, with the concurrent appearance of a new pair of signals ($\delta = 6.54$ and 6.33 ppm), whose intensities increase up to 4.0 equiv of metal ion. Resonances due to the N-lobe display a somewhat different behavior which is characteristic of intermediate/fast exchange binding to sites I and II. The $\alpha$H protons of D64 and T26 best illustrate this effect; the positions of these signals in apo-CaM ($\delta = 5.57$ and 5.53 ppm) steadily move upon addition of $Pb^{2+}$ without loss of intensity until the endpoint of the titration ($\delta = 5.64$ and 5.51 ppm). Hence, the results shown in Fig. 5 prove the coincident occupation of all four EF-hand sites of CaM by $Pb^{2+}$, although the kinetics of $Pb^{2+}$ binding to the N- and C-terminal sites are different on the $^{1}H$ time scale; this may account for the somewhat broader $^{207}Pb$ resonances observed for sites I and II (Fig. 3).

We also examined the relative binding affinities of $Pb^{2+}$ and $Cd^{2+}$ for CaM. Figure 6 shows the back titration of $(^{113}Cd^{2+})_{4.0}$ CaM with $Pb^{2+}$ monitored by $^{113}Cd$ NMR. In the absence of $Pb^{2+}$, one can detect only two $^{113}Cd$ signals ($\delta = -88.1$, $\Delta\nu_{1/2} = 75$ Hz; $\delta = -114.5$, $\Delta\nu_{1/2} = 100$ Hz) in the cadmium-loaded protein, corresponding to $^{113}Cd^{2+}$ bound to sites IV and III, respectively [31, 47]. Addition of a saturating amount of $Pb^{2+}$ to the protein leads to the complete disappearance of the $^{113}Cd$ signals, meaning that the larger metal ion quantitatively expels cadmium ion from the protein. The appearance of additional peaks in the $^{113}Cd$ spectrum during the titration is most likely

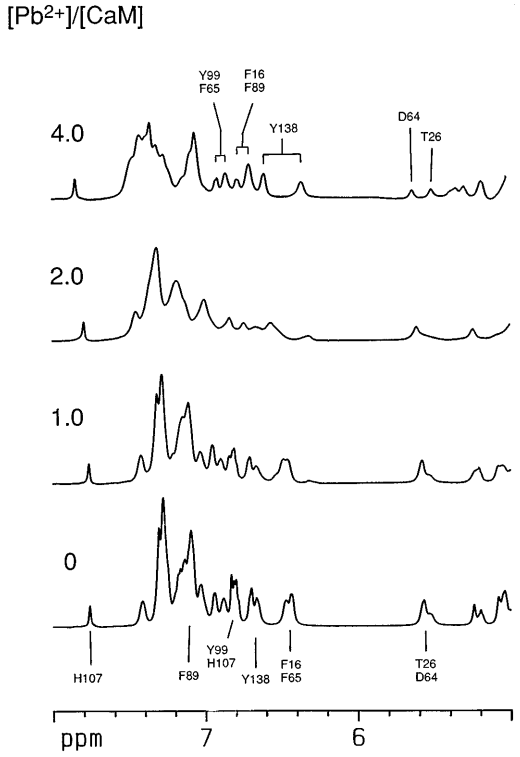


**Fig. 5** $^{1}H$ (500.139 MHz) NMR spectra of the titration of 1.37 mM bovine testis apo-CaM (150 mM KCl, $D_2O$, pH* 7.5) with $Pb^{2+}$; 1000 scans each. The assignments shown for apo-CaM, as well as tentative assignments for the $Pb^{2+}$–loaded protein, were based on analogous $^{1}H$ NMR studies of $Ca^{2+}$ and $Cd^{2+}$ binding to bovine CaM (see, for example, [47]).

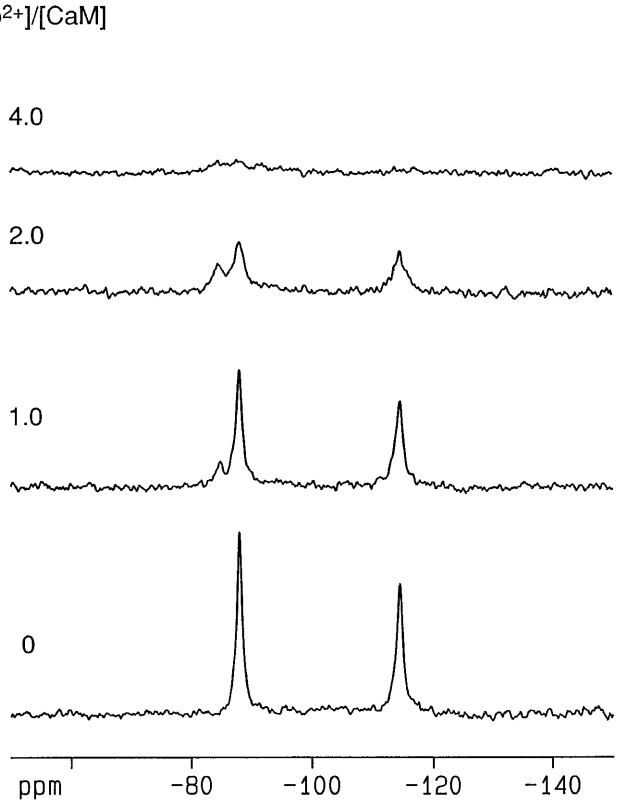


**Fig. 6** $^{113}Cd$ (110.92 MHz) NMR spectra of the back titration of 1.57 mM bovine testis $(^{113}Cd)_{4.0}$ CaM (150 mM KCl, pH 7.5) with $Pb^{2+}$; 25000 scans each

due to intersite interactions in the C-terminal lobe of the protein (see above).

The $^{207}Pb$, $^{1}H$, and $^{113}Cd$ NMR results presented in this section illuminate some significant differences between $^{207}Pb$ and the traditional probe for this class of metalloproteins, $^{113}Cd$. As observed for the parvalbumins, CaM-bound $^{207}Pb$ signals are spread out over a much larger chemical shift range ($\approx$200 ppm) than that reported in $^{113}Cd$ NMR studies of this protein ($\approx$30 ppm) [47]. However, the linewidths of the $^{207}Pb$ signals reported here are substantially larger than those for CaM-bound $^{113}Cd^{2+}$ at a magnetic field of 11.7 T (see below). Our data also indicate that there are major differences between $Pb^{2+}$ and other metal ions regarding the manner in which metal ion binding to CaM occurs. While $Pb^{2+}$ appears to show little site preference, $^{1}H$, $^{43}Ca$ and $^{113}Cd$ NMR evidence has established that $Ca^{2+}$ and $Cd^{2+}$ clearly bind to the protein in two distinct stages: stage I, high-affinity binding to sites III and IV; stage II, low-affinity binding to sites I and II [31, 32, 47–50]. In fact, the affinities of the two N-terminal sites of CaM for $Cd^{2+}$ are low enough to preclude detection of $^{113}Cd$ signals corresponding to sites I and II, due to exchange broadening [47], in contrast to the $^{207}Pb$ NMR results presented here.

## Trifluoperazine binding to CaM and $TR_2C$

Over a decade ago, Forsén and coworkers demonstrated the usefulness of $^{113}Cd$ NMR as a probe for the interaction of various drugs, including the antipsychotic drug trifluoperazine (TFP), with $^{113}Cd^{2+}$–substituted CaM [51, 52]. Recent X-ray structures of TFP complexes with the $Ca^{2+}$ form of this protein showed that the drug binds to two hydrophobic patches, one in each lobe [53, 54]. Moreover, TFP binding also imparts gross conformational changes to the protein, analogous to those found for CaM bound to, for instance, skeletal and smooth myosin light chain kinase [55, 56], thereby preventing CaM from interacting with its many target enzymes. Figure 7 shows the titration of $(^{207}Pb)_{4.0}$CaM with TFP followed by $^{207}Pb$ NMR. Upon addition of 1.0 equiv of the drug, the intensity of one of the $^{207}Pb$ signals ($\delta$ = 1082 ppm) due to the C-lobe is markedly reduced, and a new signal ($\delta$ = 1182 ppm) emerges. The other resonance from this lobe remains largely unchanged, and the signals due to sites I and II are slightly perturbed. When a further 1.0 equiv of TFP is added new resonances ($\delta$ = 965 and 854 ppm) assigned to the N-lobe of the protein emerge. Figure 7 shows that one of the C-terminal signals moved slightly upfield (to

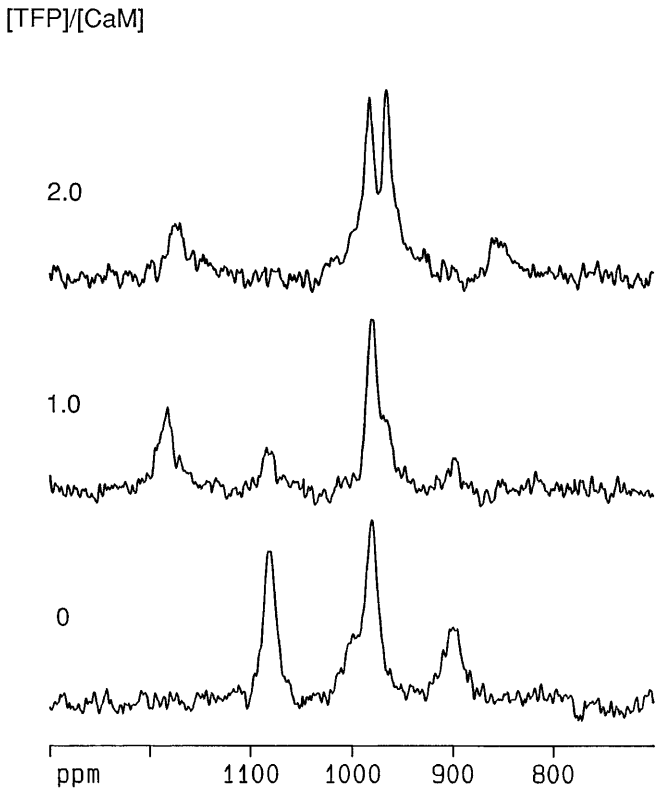


**Fig. 7** $^{207}$Pb (104.435 MHz) NMR spectra of the titration of 1.47 mM bacterially expressed mammalian $(^{207}Pb)_{4.0}$ CaM (100 mM KCl, pH 7.1) with TFP; 85000 scans each

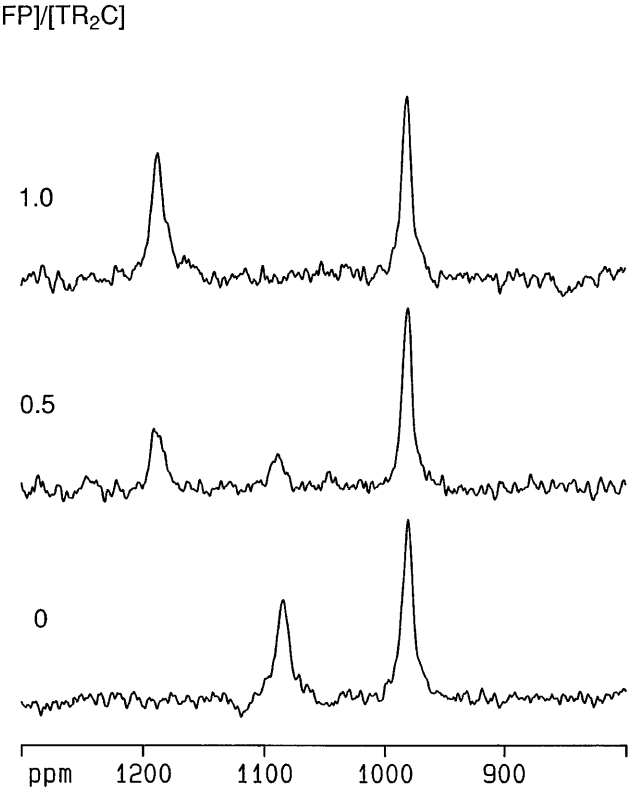


**Fig. 8** $^{207}$Pb (104.435 MHz) NMR spectra of the titration of 1.11 mM bacterially expressed mammalian $(^{207}Pb)_{2.0}$ $TR_2C$ (100 mM KCl, pH 7.2) with TFP; 60000–80000 scans each

$\delta = 1174$ ppm) and broadened at this stage of the titration. The above interpretations were confirmed by the analogous titration of $TR_2C$ (Fig. 8). Again, one observes slow exchange binding of 1.0 equiv of the drug to the half-molecule, and only the lower-field signal is altered during the experiment. The $^{207}$Pb NMR data for the $^{207}Pb^{2+}$ forms of CaM and $TR_2C$ in the presence of a saturating amount of TFP are also listed in Table 3.

Some parallels and differences with analogous $^{113}$Cd NMR studies of TFP binding to CaM can be drawn [32, 47]. As was observed by $^{113}$Cd NMR, the interaction of TFP to $(^{207}Pb)_{4.0}$CaM proceeds primarily in a sequential manner, with binding first to the C-lobe and subsequently the N-lobe. In addition, one observes chemical shift differences for practically all of the signals, meaning that conformational changes imparted by binding of the drug to both lobes of the protein are sensed by all four binding sites. This effect has also been documented for the $^{113}Cd^{2+}$–form of CaM. However, our results indicate that binding of TFP produces no appreciable reductions in the linewidths of the CaM-bound $^{207}$Pb signals. In contrast, the binding of this and other drugs in general significantly reduce the exchange rates of bound $^{113}Cd^{2+}$, especially in sites I and II, which facilitates the detection of bound cadmium in these sites [47, 51, 52].

## Field dependence of CaM-bound $^{207}$Pb and $^{113}$Cd NMR signals

The linewidths of the $^{207}$Pb and $^{113}$Cd NMR signals for $(^{207}Pb)_{4.0}$CaM $(TFP)_{2.0}$ and $(^{113}Cd)_{4.0}$CaM were obtained at a number of magnetic fields. At each field, the CaM-bound $^{207}$Pb resonances were substantially broader than the analogous $^{113}$Cd peaks, and the linewidths of the former exhibited a marked dependence on the square of the magnetic field (Fig. 9). This $B_0^2$ dependence is quite diagnostic of nuclear relaxation via the chemical shift anisotropy mechanism [57], which is quite common in $^{207}$Pb NMR particularly at high fields, due to the vast chemical shift range of this nucleus [20]. The detrimental effect of CSA on signal resolution and detectability is in fact a general concern in protein NMR studies involving other third-row ("heavy") $I = {}^1/_2$ metal nuclei, such as $^{199}$Hg and $^{205}$Tl, where very broad resonances have been reported [58, 59]. However, as has been demonstrated in $^{113}$Cd NMR studies of calbindin $D_{9K}$ and $\alpha$-lactalbumins, one cannot neglect the contribution of exchange processes, which are also characterized by a $B_0^2$ dependence, to the $T_2$ relaxation (inversely proportional to linewidth) of protein-bound metal nuclei [33, 60]. In the absence of a chemical shift anisotropy ($\sigma$) value for a compara-

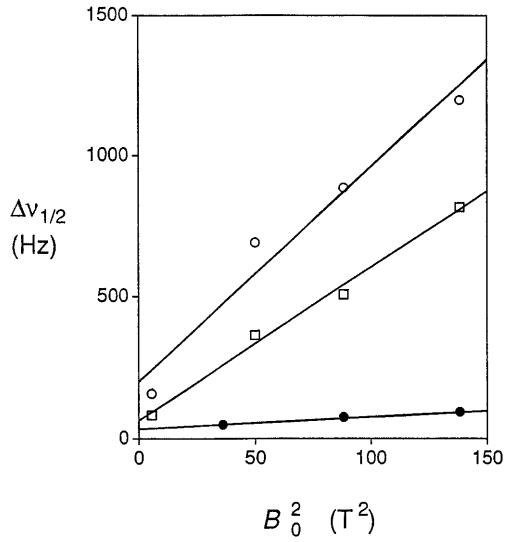


**Fig. 9** Dependence of the CaM-bound $^{207}$Pb and $^{113}$Cd signal linewidths on the square of the magnetic field strength. ○ Bovine testis ($^{207}$Pb)$_{4.0}$CaM(TFP)$_{2.0}$, signal at $\delta$ = 983 ppm (site III or IV); □ bovine testis ($^{207}$Pb)$_{4.0}$CaM(TFP)$_{2.0}$, signal at $\delta$ = 965 ppm (site I or II); ● bovine testis ($^{113}$Cd)$_{4.0}$CaM, $\delta$ = –114.5 ppm (site III). The approximate linewidth for the C-terminal sites (III and IV) of CaM at 6.0 T was obtained from [46]

ble coordination complex of $Pb^{2+}$, one must have knowledge of the longitudinal relaxation ($T_1$) times for the protein-bound $^{207}$Pb signals in order to establish the relative contributions of these two effects to the observed linewidths. Consequently, we obtained $T_1$ values for the signals due to $^{207}Pb^{2+}$ bound to the two helix-loop-helix sites in $TR_2C$ at a field strength of 9.4 T. Assuming that no other magnetic relaxation processes contribute to the observed longitudinal relaxation times, one can use Eq. 1 to calculate $\sigma$, and subsequently insert these values into Eq. 2 to obtain the $T_2{}^{CSA}$ for both signals. The results are given in Table 4. For both signals, CSA failed to entirely account for the observed linewidth, meaning that other effects are present. Indeed, we found that the linewidths of both signals for $TR_2C$, particularly the downfield peak, increased with increasing temperature, indicative of the presence of exchange (data not shown).

**Table 4** $T_1$ and $T_2$ relaxation data for $TR_2C$-bound $^{207}$Pb signals at 9.4 T (all data obtained using the TFP complex of $^{207}Pb_2$-$TR_2C$)

| δ (ppm) | $T_1$ (ms) | σ (ppm) | $T_2^{CSA}$ (ms)[a] | $T_2^{eff}$ (ms)[b] |
|---|---|---|---|---|
| 1187 | 14 | 1910 | 1.66 | 0.38 |
| 981 | 27 | 1380 | 3.20 | 0.54 |

[a] Calculated using Eqs. 1 and 2 assuming a $\tau_c$ of 6.3 ns [61]
[b] Calculated from the observed linewidths according to the relation: $T_2^{eff} = \frac{1}{\pi \Delta\nu_{1/2}}$

$$1/T_1{}^{CSA} = 2/15\ \omega_0{}^2\Delta\sigma^2\ \{\tau_c/(1+\omega_0{}^2\tau_c{}^2)\} \quad (1)$$

$$1/T_2{}^{CSA} = 1/15\ \omega_0{}^2\Delta\sigma^2\ \{4/3\ \tau_c\ +\ \tau_c/(1+\omega_0{}^2\tau_c{}^2)\} \quad (2)$$

## Conclusions

The results presented in this article constitute, to our knowledge, the first $^{207}$Pb NMR studies of metalloproteins. Two key intrinsic properties of $^{207}$Pb make this nucleus an attractive novel probe for the study of metal ion binding sites in proteins. First, on a number of occasions in this paper we have alluded to the huge chemical shift range exhibited by $^{207}$Pb and the sensitivity of this parameter to variations in the chemical environment of the metal nucleus. $^{207}$Pb chemical shift data accumulated for complexes to date indicate that increasing the polarizability of the coordinating ligand tends to decrease the nuclear shielding (i.e., S<N<O); an effect analogous to that known for $^{113}$Cd, albeit on a much larger scale [20]. For example, the introduction of two nitrogen ligands into the coordination sphere of the metal ion in $[Pb(EDTA)]^{2-}$ produces an extraordinary downfield shift in the $^{207}$Pb signal ($\delta \approx 2350$ ppm) [62]. Hence, one can easily envisage applying $^{207}$Pb NMR to the study of metal ion binding sites in proteins which contain softer ligands (e.g., His, Cys) analogous to the large body of $^{113}$Cd NMR studies on a variety of proteins [16–18]. Second, like other heavy I = $^1/_2$ metal nuclei, $^{207}$Pb can exhibit quite large through-bond couplings to nearby I = $^1/_2$ nuclei [20]. This opens the possibility of using inverse ($^1$H, $^{207}$Pb) and isotope filtering techniques to detect the residues directly involved in coordinating the metal ion. Such approaches have been applied to proteins in which three-bond $^1$H, X couplings are primarily involved, where X = $^{113}$Cd [63–66], $^{109}$Ag [67], even $^{199}$Hg [58], in spite of broad protein-bound signals (i.e., up to $10^3$ Hz). However, the lack of spin-spin coupling between, for example, $^{113}$Cd and protons four bonds away on carbons adjacent to ligating carboxylates have thus far precluded the application of these techniques to $Ca^{2+}$–binding proteins. Hence, it would be particularly appealing to perform such experiments on $^{207}$Pb-substituted $Ca^{2+}$–binding proteins; projects to this end are currently under way in our laboratory.

The results presented in this article should also alert the reader to some important experimental considerations that should be kept in mind in biomolecular $^{207}$Pb NMR studies. For example, the large chemical shift range for this nucleus requires one to employ quite large sweep widths during data acquisition, which may lead to unequal excitation of widely spaced signals in the same spectrum. Moreover, the larger signal linewidths typically observed for this heavy nucleus make it intrinsically less sensitive than other probes (e.g., $^{113}$Cd); however, this is to some extent off-set by the short protein-bound $T_1$ values (i.e., decreased repeti-

tion times). In spite of such difficulties, we feel that the importance of $Pb^{2+}$ in toxicology, particularly its propensity for mimicking the many physiological functions of $Ca^{2+}$ [22], make $^{207}Pb$ NMR a potentially valuable means of studying biologically relevant macromolecules.

**Acknowledgements** This research project was sponsored by an operating grant from the Medical Research Council of Canada (MRC). J.M.A. and T.Y. were supported by studentships from the Natural Sciences and Engineering Research Council of Canada, and the Alberta Heritage Foundation for Medical Research (AHFMR). H.J.V. acknowledges salary support from the AHFMR. The NMR spectrometers used in this work (University of Calgary) were purchased with funds provided by the AHFMR and MRC. We are indebted to Dr. A.S. Tracey (Simon Fraser University), Dr. M.W. Germann (now at Thomas Jefferson University), and Dr. S. Mooibroek (now at University of Waterloo) for their assistance in performing the lower-field $^{207}Pb$ NMR work. Finally, we would like to thank Dr. D.D. McIntyre (University of Calgary) for spectrometer upkeep.

## References

1. Lippard SJ, Berg JM (1994) Principles of bioinorganic chemistry. University Science Books, Mill Valley, Calif
2. da Silva JJRF, Williams RJP (1991) The biological chemistry of the elements. Clarendon Press, Oxford
3. Heizmann CW, Hunziker W (1991) Intracellular calcium-binding proteins: more sites than insights. Trends Biochem Sci 16:98–103
4. Hiraoki T, Vogel HJ (1987) Structure and function of calcium-binding proteins. J Cardiovasc Pharmacol 10:S14–S31
5. McPhalen CA, Strynadka NCJ, James MNG (1991) Calcium-binding sites in proteins: a structural perspective. Adv Protein Chem 42:77–144
6. Strynadka NCJ, James MNG (1989) Crystal structures of the helix-loop-helix calcium-binding proteins. Annu Rev Biochem 58:951–998
7. Swain AL, Kretsinger RH, Amma EL (1989) Restrained least squares refinement of native (calcium) and cadmium-substituted carp parvalbumin using X-ray crystallographic data at 1.6-Å resolution. J Biol Chem 264:16620–16628
8. Kumar VD, Lee L, Edwards BFP (1990) Refined crystal structure of calcium-liganded carp parvalbumin 4.25 at 1.5-Å resolution. Biochemistry 29:1404–1414
9. Padilla A, Vuister GW, Boelens R, Kleywegt GJ, Cavé A, Parello J, Kaptein R (1990) Homonuclear three-dimensional $^{1}H$ NMR spectroscopy of pike parvalbumin. Comparison of short- and medium-range NOEs from 2D and 3D NMR. J Am Chem Soc 112:5024–5030
10. Vogel HJ (1994) Calmodulin: a versatile calcium mediator protein. Biochem Cell Biol 72:357–376
11. Means AR, van Berkum MFA, Bagchi I, Lu KP, Rasmussen CD (1991) Regulatory functions of calmodulin. Pharmacol Ther 50:255–270
12. Babu YS, Sack JS, Greenhough TJ, Bugg CE, Means AR, Cook WJ (1985) Three-dimensional structure of calmodulin. Nature 315:37–40
13. Babu YS, Bugg CE, Cook WJ (1988) Structure of calmodulin refined to 2.2 Å. J Mol Biol 204:191–204
14. Chattopadhyaya R, Meador WE, Means AR, Quiocho FA (1992) Calmodulin structure refined at 1.7 Å resolution. J Mol Biol 228:1177–1192
15. Forsén S, Johansson C, Linse S (1993) Calcium nuclear magnetic resonance. Methods Enzymol 227:107–118
16. Vogel HJ, Forsén S (1987) NMR studies of calcium-binding proteins. In: Berliner LJ, Reuben J (eds) Biological magnetic resonance, vol 7. Plenum Press, New York, pp 249–309
17. Coleman JE (1993) Cadmium-113 nuclear magnetic resonance applied to metalloproteins. Methods Enzymol 227:16–43
18. Summers MF (1988) $^{113}Cd$ NMR spectroscopy of coordination compounds and proteins. Coord Chem Rev 86:43–134
19. Shannon RD (1976) Revised effective ionic radii and systematic studies of interatomic distances in halides and chalcogenides. Acta Crystallogr A32:751–767
20. Wrackmeyer B, Horchler K (1989) $^{207}Pb$-NMR parameters. Annu Rep NMR Spectrosc 22:249–304
21. Brevard C, Granger P (1981) Handbook of high resolution multinuclear NMR. Wiley, New York
22. Goldstein GW (1993) Evidence that lead acts as a calcium substitute in secondary messenger metabolism. Neurotoxicology 14:97–102
23. Fullmer CS, Edelstein S, Wasserman RH (1985) Lead-binding properties of intestinal calcium-binding proteins. J Biol Chem 260:6816–6819
24. Long GJ, Rosen JF, Schanne FAX (1994) Lead activation of protein kinase C from rat brain. J Biol Chem 269:834–837
25. Chao S-H, Suzuki Y, Zysk JR, Cheung WY (1984) Activation of calmodulin by various metal cations as a function of ionic radius. Mol Pharmacol 26:75–82
26. Chao SH, Bu CH, Cheung WY (1995) Stimulation of myosin light-chain kinase by $Cd^{2+}$ and $Pb^{2+}$. Arch Toxicol 69:197–203
27. Pechère J-F, Demaille J, Capony J-P (1971) Muscular parvalbumins: preparative and analytical methods of general applicability. Biochim Biophys Acta 236:391–408
28. Yagi K, Matsuda S, Nagamoto H, Mikuni T, Yazawa M (1982) Structure and $Ca^{2+}$–dependent conformational change of calmodulin. In: Kakiuchi S, Hidaka H, Means AR (eds) Calmodulin and intracelluar $Ca^{2+}$ receptors. Plenum Press, New York, pp 75–91
29. Yazawa M, Sakuma M, Yagi K (1980) Calmodulins from muscles of marine invertebrates, scallop and sea anemone. J Biochem 87:1313–1320
30. Zhang M, Vogel HJ (1993) Determination of the side chain $pK_a$ values of the lysine residues in calmodulin. J Biol Chem 268:22420–22428 and references therein
31. Andersson A, Forsén S, Thulin E, Vogel HJ (1983) Cadmium nuclear magnetic resonance studies of the proteolytic fragments of calmodulin: assignment of strong and weak cation binding sites. Biochemistry 22:2309–2313
32. Thulin E, Andersson A, Drakenberg T, Forsén S, Vogel HJ (1984) Metal ion and drug binding to proteolytic fragments of calmodulin: proteolytic, cadmium-113, and proton nuclear magnetic resonance studies. Biochemistry 23:1862–1870
33. Aramini JM, Hiraoki T, Yue Ke, Nitta K, Vogel HJ (1995) Cadmium-113 NMR studies of bovine and human $\alpha$-lactalbumin and equine lysozyme. J Biochem Tokyo 117:623–628
34. Bjornson ME, Corson DC, Sykes BD (1985) $^{13}C$ and $^{113}Cd$ NMR studies of the chelation of metal ions by the calcium binding protein parvalbumin. J Inorg Biochem 25:141–149
35. Cavé A, Saint-Yves A, Parello J, Swärd M, Thulin E, Lindman B (1982) NMR studies on parvalbumin phylogeny and ionic interactions. Mol Cell Biochem 44:161–172
36. Watterson DM, Harrelson Jr WG, Keller PM, Sharief F, Vanaman TC (1976) Structural similarities between the $Ca^{2+}$–dependent regulatory proteins of 3':5′-cyclic nucleotide phosphodiesterase and actomysin ATPase. J Biol Chem 251:4501–4513
37. Itakura M, Iio T (1992) Static and kinetic studies of calmodulin and melittin complex. J Biochem Tokyo 112:183–191
38. Aramini JM, Drakenberg T, Hiraoki T, Yue Ke, Nitta K, Vogel HJ (1992) Calcium-43 NMR studies of calcium-binding lysozymes and $\alpha$-lactalbumins. Biochemistry 31:6761–6768

39. DrakenbergT, Lindman B, Cavé A, Parello J (1978) Non-equivalence of the CD and EF sites of muscular parvalbumins: a $^{113}$Cd NMR study. FEBS Lett 92:346–350
40. Drakenberg T, Swärd M, Cavé A, Parello J (1985) Metal-ion binding to parvalbumin. Biochem J 227:711–717
41. Vogel HJ, Drakenberg T, Forsén S, O'Neil JDJ, Hofmann T (1985) Structural differences in the two calcium binding sites of porcine intestinal calcium binding protein: a multinuclear NMR study. Biochemistry 24:3870–3876
42. Cavé A, Parello J, Drakenberg T, Thulin E, Lindman B (1979) $Mg^{2+}$ binding to parvalbumins studied by $^{25}$Mg and $^{113}$Cd NMR spectroscopy. FEBS Lett 100:148–152
43. Dalgarno DC, Klevit RE, Levine BA, Williams RJP, Dobrowolski Z, Drabikowski W (1984) $^{1}$H NMR studies of calmodulin. Resonance assignments by use of tryptic fragments. Eur J Biochem 138:281–289
44. Ikura M, Hiraoki T, Hikichi K, Minowa O, Yamaguchi H, Yazawa M, Yagi K (1984) Nuclear magnetic resonance studies on calmodulin: $Ca^{2+}$–dependent spectral change of proteolytic fragments. Biochemistry 23:3124–3128
45. Martin SR, Bayley PM (1986) The effects of $Ca^{2+}$ and $Cd^{2+}$ on the secondary and tertiary structure of bovine testis calmodulin. Biochem J 238:485–490
46. Fabian H, Yuan T, Vogel HJ, Mantsch HH (1996) Comparative analysis of the amino- and carboxy-terminal domains of calmodulin by Fourier Transform Infrared spectroscopy. Eur Biophys J (in press)
47. Forsén S, Thulin E, Drakenberg T, Krebs J, Seamon KA (1980) $^{113}$Cd NMR study of calmodulin and its interaction with calcium, magnesium and trifluoperazine. FEBS Lett 117:189–194
48. Klevit RE, Dalgarno DC, Levine BA, Williams RJP (1984) $^{1}$H NMR studies of calmodulin: the nature of the $Ca^{2+}$–dependent conformational change. Eur J Biochem 139:109–114
49. Ikura M, Hiraoki T, Hikichi K, Mikuni T, Yazawa M, Yagi K (1983) Nuclear magnetic resonance studies on calmodulin: calcium-induced conformational change. Biochemistry 22:2573–2579
50. Andersson T, Drakenberg T, Forsén S, Thulin E, Swärd M (1982) Direct observation of $^{43}$Ca NMR signals from $Ca^{2+}$ ions bound to proteins. J Am Chem Soc 104:576–580
51. Andersson A, Drakenberg T, Thulin E, Forsén S (1983) A $^{113}$Cd and $^{1}$H NMR study of the interaction of calmodulin with D600, trifluoperazine and some other hydrophobic drugs. Eur. J. Biochem 134:459–465
52. Andersson A, Drakenberg T, Forsén S (1985) The interaction of various drugs with calmodulin as monitored by $^{113}$Cd NMR. In: Hidaka H, Hartshorn DJ (eds) Calmodulin antagonists and cellular physiology. Academic Press, New York, pp 27–44
53. Vandonselaar M, Hickie RA, Quail JW, Delbaere LTJ (1994) Trifluoperazine-induced conformational change in $Ca^{2+}$–calmodulin. Nature Struct Biol 1:795–800
54. Cook WJ, Walter LJ, Walter MR (1994) Drug binding by calmodulin: crystal structure of a calmodulin-trifluoperazine complex. Biochemistry 33:15259–15265
55. Ikura M, Clore M, Gronenborn A, Zhu G, Klee CB, Bax A (1992) Solution structure of a calmodulin-target peptide complex by multidimensional NMR. Science 256:632–637
56. Meador WE, Means AR, Quiocho FA (1992) Target enzyme recognition by calmodulin: 2.4 Å structure of a calmodulin-peptide complex. Science 257:1251–1255
57. Farrar TC, Becker ED (1971) Pulse and Fourier transform NMR. Academic Press, New York, pp 46–65
58. Utschig LM, Bryson JW, O'Halloran TV (1995) Mercury-199 NMR of the metal receptor site in MerR and its protein-DNA complex. Science 268:380–385
59. Aramini JM, Krygsman PH, Vogel HJ (1994) Thallium-205 and carbon-13 NMR studies of human sero- and chicken ovotransferrin. Biochemistry 33:3304–3311
60. Kördel J, Johansson C, Drakenberg T (1992) $^{113}$Cd NMR relaxation study of the protein calbindin $D_{9K}$. J Magn Reson 100:581–587
61. Barbato G, Ikura M, Kay LE, Pastor RW, Bax A (1992) Backbone dynamics of calmodulin studied by $^{15}$N relaxation using inverse detected two-dimensional NMR spectroscopy: the central helix is flexible. Biochemistry 31:5269–5278
62. Nakashima TT, Rabenstein DL (1983) A lead-207 nuclear magnetic resonance study of the complexation of lead by carboxylic acids and aminocarboxylic acids. J Magn Reson 51:223–232
63. Otvos JD, Engeseth HR, Wehrli S (1985) Multiple-quantum $^{113}$Cd-$^{1}$H correlation spectroscopy as a probe of metal coordination environments in metallo-proteins. J Magn Reson 61:579–584
64. Frey MH, Wagner G, Vašák M, Sørensen OW, Neuhaus D, Wörgötter E, Kägi JHR, Ernst RR, Wüthrich K (1985) Polypetide-metal cluster connectivities in metallothionein 2 by novel $^{1}$H-$^{113}$Cd two-dimensional NMR experiments. J Am Chem Soc 107:6847–6851
65. Wörgötter E, Wagner G, Vašák M, Kägi JHR, Wüthrich K (1988) Heteronuclear filters for two-dimensional $^{1}$H NMR. Identification of the metal-bound amino acids in metallothionein and observation of small heteronuclear long-range couplings. J Am Chem Soc 110:2388–2393
66. Pan T, Coleman JE (1990) GAL4 transcription factor is not a zinc finger but forms a $Zn(II)_2Cys_6$ binuclear cluster. Proc Natl Acad Sci USA 87:2077–2081
67. Narula SS, Mehra RK, Winge DR, Armitage IM (1991) Establishment of the metal-to-cysteine connectivities in silver-substituted metallothionein. J Am Chem Soc 113:9354–9358